Supplementary Figure S1: Detection of VEGFR3 tyrosine phosphorylation using proximity ligation assay after VEGF-C injection.

(A-D) Representative LSM images of proximity ligation assays (PLA) on cross-sections through the jugular lymph sacs (jls) of (A, B) wild type E11.5 mouse embryos or (C, D) mouse embryos injected with VEGF-C (C156S), and cultivated for 30 minutes in whole embryo culture (WEC). Red staining (arrowheads) indicates sites of VEGFR3 with phosphorylated tyrosines. A co-staining is shown for the lymphatic marker Lyve-1 (green) and nuclei (DAPI, blue). Scale bars, 10 μm.

(E) Increase in sites of VEGFR3 with phosphorylated tyrosines in LECs of wild type E11.5 mouse embryos injected with VEGF-C (C156S) (grey column) compared to untreated mouse embryos (black column). All values are means ± SD, n = 3 embryos per condition, *$p < 0.05$ ($p = 0.029$).

Supplementary Figure S2: 'Loss-of-fluid' experiments: Removal of interstitial fluid from mouse embryos.

(A) Bright field image of an E11.5 wild type mouse embryo. The area indicated is magnified in (B) and (C).

(B, B') A glass micro-capillary was inserted into the jugular mesenchyme of an E11.5 wild type mouse embryo, and 10 nl interstitial fluid were removed. (B') Magnification of (B). The bracket indicates the amount (10 nl) of interstitial fluid removed using the glass capillary.

(C, C') A glass micro-capillary was inserted into the jugular mesenchyme of an E11.5 wild type mouse embryo, and 100 nl interstitial fluid were removed. (C') Magnification of (C). The bracket indicates the amount (100 nl) of interstitial fluid removed using the glass capillary.

(D, D') Interstitial fluid removed using the glass capillary and stained with the nuclear marker Hoechst. (D') Image of fluid containing cells stained with Hoechst to visualize the cell nuclei (positive control). Note the absence of cell nuclei in (D) compared to (D').

Supplementary Figure S3: 'Gain-of-fluid' experiments: Injection of interstitial fluid increases LEC proliferation.

(A-D) Cross-sections through the jugular lymph sac (jls) of representative wild type E11.5 mouse embryos injected with (A, B) 10 nl interstitial fluid or (C, D) 100 nl interstitial fluid, and immunostained for Lyve-1 (green), proliferation marker phospho-histone H3 (red) and nuclei (DAPI, blue). Proliferating cells are indicated (arrows). Scale bars, (A, C) 100 μm, (B, D) 20 μm.

(E) Increase in LEC proliferation in wild type E11.5 mouse embryos injected with 10 nl interstitial fluid (dark grey column) or 100 nl interstitial fluid (light grey column) compared to untreated wild type E11.5 mouse embryos (black column). All values are means ± SD, $n \geq 3$ embryos per condition, $^*p < 0.05$ (first bracket: $p = 0.011$, second bracket: $p = 0.035$).

Supplementary Figure S4: In the jugular region of E12.0 embryos, β1 integrin is highly expressed in LECs and VECs, whereas VEGFR3 is mainly expressed in LECs.

(A, B) Cross-sections through a jugular lymph sac (jls) of a representative wild type E12.0 mouse embryo immunostained for (A) VEGFR2 or (B) VEGFR3 (green), β1 integrin (red) and nuclei (DAPI, blue). Anterior cardinal vein (acv) and dorsal aorta (da) are indicated. Scale bars, 200 µm.

(C-E) Magnified region of (A): LECs of the jugular lymph sac (jls) immunostained for (C) VEGFR2 (green), (D) β1 integrin (red), and (E) merged with nuclei (DAPI, blue). Scale bar, 10 µm.

(F-H) Magnified region of (A): VECs immunostained for (F) VEGFR2 (green), (G) β1 integrin (red), and (H) merged with nuclei (DAPI, blue). Scale bar, 10 µm.

(I-K) Magnified region of (B): LECs of the jugular lymph sac (jls) immunostained for (I) VEGFR3 (green), (J) β1 integrin (red), and (K) merged with nuclei (DAPI, blue). Scale bar, 10 µm.

(L-N) Magnified region of (B): VECs immunostained for (L) VEGFR3 (green), (M) β1 integrin (red), and (N) merged with nuclei (DAPI, blue). Note the absence of VEGFR3 expression in VECs. Scale bar, 10 µm.

Supplementary Figure S5: 'Gain-of-fluid' experiments: Increasing interstitial fluid volume does not enhance VEGFR2 tyrosine phosphorylation in LECs.

(A-D) Representative LSM images of proximity ligation assays (PLA) on cross-sections through the jugular lymph sacs (jls) of wild type E11.5 mouse embryos injected with (A, B) 4.2 nl PBS or (C, D) 34 nl PBS, and cultivated for 30 minutes in whole embryo culture (WEC). Red staining (arrowheads) indicates PLA sites of VEGFR2 with phosphorylated tyrosines. A co-staining is shown for the lymphatic marker Lyve-1 (green) and nuclei (DAPI, blue). Scale bars, (A, C) 20 µm, (B, D) 10 µm.

(E) Lack of increase in the number of PLA sites of VEGFR2 with phosphorylated tyrosines in LECs of wild type E11.5 mouse embryos injected with 4.2 nl PBS (dark grey column) or 34 nl PBS (light grey column) compared to untreated wild type E11.5 mouse embryos (black column). All values are means ± SD, n ≥ 4 embryos per condition, ns = non-significant (first bracket: $p = 0.878$, second bracket: $p = 0.982$).

Supplementary Figure S6: 'Gain-of-fluid' experiments: Increasing interstitial fluid volume does not enhance VEC proliferation.

(A, A', B, B') LSM images of cross-sections through representative E11.5 wild type mouse embryos injected with (A) 4.2 nl PBS or (B) 34 nl PBS, and immunostained for proliferation marker phospho-histone H3 (green), PECAM-1 (red), and nuclei (DAPI, blue). Open arrows point to proliferating vascular endothelial cells (VECs), some of which are magnified in A' and B'. Anterior cardinal vein (acv) and dorsal aorta (da) are indicated. Scale bars, (A, B) 100 μm, (A', B') 10 μm.

(C) Lack of increase in VEC proliferation in wild type E11.5 mouse embryos injected with 4.2 nl PBS (dark grey column) or 34 nl PBS (light grey column) compared to untreated wild type E11.5 mouse embryos (black column). All values are means ± SD, n = 3 embryos per condition, ns = non-significant (first bracket: $p = 0.915$, second bracket: $p = 0.567$).

Supplementary Figure S7: 'Gain-of-fluid' experiments: Increasing interstitial fluid volume enhances the activation of β1 integrin, and its interaction with VEGFR3.

(A, B, E, F) Representative LSM images of cross-sections through jugular lymph sacs (jls) of E11.5 wild type mouse embryos injected with (A, B) 4.2 nl PBS or (E, F) 34 nl PBS, and immunostained for VEGFR3 (green), activated β1 integrin (red) and nuclei (DAPI, blue). Scale bars, 10 μm.

(C, G) Masks of the VEGFR3 staining of images (B) and (F) superimposed on the 'activated β1 integrin' channel. The fluorescence intensity of this specific region was measured in (M). Note the increase in intensity of activated β1 integrin in embryos injected with (G) 34 nl PBS, compared to the injection of (C) 4.2 nl PBS.

(D, H) Colocalised pixels of the staining of VEGFR3 and activated β1 integrin from (B) and (F). Note the increased colocalisation in embryos injected with (H) 34 nl PBS, compared to the injection of (D) 4.2 nl PBS.

(I-L) Representative LSM images of proximity ligation assays (PLA) on cross-sections through the jugular lymph sacs (jls) of wild type E11.5 mouse embryos injected with (I, J) 4.2 nl PBS or (K, L) 34 nl PBS, and cultivated for 30 minutes in whole embryo culture (WEC). Red staining (arrowheads) shows PLA sites indicating an interaction between VEGFR3 and β1 integrin. A co-staining is shown for the lymphatic marker Lyve-1 (green) and nuclei (DAPI, blue). Scale bars, 20 μm.

(M) Increase in fluorescence intensity of the staining for activated β1 integrin in LECs of wild type E11.5 mouse embryos injected with 4.2 nl PBS (dark grey column) or 34 nl PBS (light grey column) compared to untreated wild type E11.5 mouse embryos (black column). All values are means ± SD, n ≥ 3 embryos per condition, *p < 0.05 (first bracket: p = 0.049, second bracket: p = 0.030).

(N) Increase in colocalisation of VEGFR3 with activated β1 integrin in LECs of wild type E11.5 mouse embryos injected with 4.2 nl PBS (dark grey column) or 34 nl PBS (light grey column) compared to untreated wild type E11.5 mouse embryos (black column). All values are means ± SD, n ≥ 3 embryos per condition, *p < 0.05 (first bracket: p = 0.030, second bracket: p = 0.026).

(O) Increase in sites of PLA between VEGFR3 and β1 integrin in LECs of wild type E11.5 mouse embryos injected with 4.2 nl PBS (dark grey column) or 34 nl PBS (light grey column) compared to untreated wild type E11.5 mouse embryos (black column). All values are means ± SD, n = 3 embryos per condition, *p < 0.05 (first bracket: p = 0.036, second bracket: p = 0.046).

Supplementary Figure S8: Stretching LECs increases colocalisation of VEGFR3 with β1 integrin, and enhances the activation of β1 integrin.

(A, B) Representative LSM images of human LECs that were (A) non-stretched and (B) stretched. The LECs were fixed after removal from the stretching chamber, and immunostained for activated β1 integrin (green) and nuclei (DAPI, blue). Scale bars, 10 μm.

(C) Increase in fluorescence intensity of activated β1 integrin in LECs that were non-stretched and stretched. All values are means ± SD, n ≥ 20 cells per condition in 3 experiments, *p = 0.042.

(D-F) Representative LSM images of human LECs immunostained for VEGFR3 (green), β1 integrin (red) and nuclei (DAPI, blue). Representative images of (D) a non-stretched LEC, (E) an LEC stretched after transfection with RLuc control siRNA, and (F) an LEC stretched after transfection with β1 integrin siRNA. Arrowheads (E) point to sites where VEGFR3 and β1 integrin colocalise. Scale bars, 10 μm.

(G) Increase in colocalisation of VEGFR3 with β1 integrin in LECs that were non-stretched, stretched after transfection with RLuc control siRNA or stretched after transfection with β1 integrin siRNA. All values are means ± SD, n = 50 cells, *p = 0.043, ns = non-significant (p = 0.957).

(H-J) Representative LSM images of proximity ligation assays (PLA) on human LECs that were (H) non-stretched, (I) stretched, and (J) stretched in

the presence of VEGF-C. Red staining indicates sites of interaction between VEGFR3 and β1 integrin. Scale bars, 10 μm.

(K) Increase in sites of PLA between VEGFR3 and β1 integrin in LECs that were non-stretched, non-stretched in the presence of VEGF-C, stretched, or stretched in the presence of VEGF-C. All values are means ± SD, n > 70 cells per condition in 3 experiments, *p < 0.05 (first bracket: p = 0.035, second bracket: p = 0.009).

(L-O) Representative LSM images of (L, M) non-stretched LECs and (N, O) stretched LECs immunostained for F-actin (green), β1 integrin (red) and nuclei (DAPI, blue). Scale bars, 10 μm.

Supplementary Figure S9: Stretching LECs increases VEGFR3 tyrosine phosphorylation in a β1 integrin-dependent manner as determined by phospho-VEGFR3 ELISA.

(A-C) Representative DIC live-cell images of (A) non-stretched human LECs, (B) human LECs stretched after transfection with RLuc control siRNA, and (C) human LECs stretched after transfection with β1 integrin siRNA-1, giving a 70 to 80 % knockdown of the β1 integrin protein (data not shown). Nuclei were artificially coloured. Scale bars, 10 μm.

(D) Increase in cell length, and nuclear length (hatched columns), of human LECs that were non-stretched (white columns), stretched after transfection with RLuc control siRNA (black columns) or stretched after transfection with β1 integrin siRNA-1 (grey columns). All values are means ± SD, n = 50 cells, *$p < 0.05$ (cell length, first bracket: $p = 0.0006$, second bracket: $p = 0.0002$; nuclear length, first bracket: $p = 0.042$, second bracket: $p = 0.046$).

(E) Increase in VEGFR3 tyrosine phosphorylation in LECs that were non-stretched (white columns), stretched (black columns) or stretched after β1 integrin silencing (grey columns). The LECs were transfected with control siRNA, β1 integrin siRNA-1, β1 integrin siRNA-2 targeting the 3'-UTR, or β1 integrin siRNA-2 together with a 3'-EGFP-β1 integrin expression vector (rescue), and cell lysates were analysed by ELISA after 30 minutes stretching. All values are means ± SEM, $n \geq 3$ experiments, *$p < 0.05$ (first bracket: $p = 0.025$, second bracket: $p = 0.028$, third bracket: $p = 0.010$, fourth bracket: p =

0.017, fifth bracket: p = 0.037, last bracket: p = 0.001, lower bracket: p = 0.044).

(F) Increase in VEGFR3 tyrosine phosphorylation in LECs grown on polyacrylamide gels of different stiffness functionalized with fibronectin. All values are means ± SD, n ≥ 3 gels per condition, *p < 0.05 (first bracket: p = 0.037, second bracket: p = 0.001).

Supplementary Figure S10: Stretching LECs increases VEGFR3 tyrosine phosphorylation as indicated by proximity ligation assays.

(A-D) Representative LSM images of proximity ligation assays (PLA) on human LECs that were (A) non-stretched, (B) non-stretched in the presence of VEGF-C, (C) stretched, and (D) stretched in the presence of VEGF-C. The LECs were fixed after removal from the stretching chamber, and immunostained. Red staining indicates sites of VEGFR3 with phosphorylated tyrosines. Scale bars, 10 μm.

(E) Increase in VEGFR3 tyrosine phosphorylation as indicated by PLA (A-D). All values are means ± SD, n > 50 cells per condition in 3 experiments, *$p < 0.05$ (first bracket: $p = 0.00002$, second bracket: $p = 0.043$, third bracket: $p = 0.049$).

Supplementary Figure S11: Stretching LECs increases cell proliferation in a β1 integrin- and VEGFR3-dependent manner.

(A-D) Representative images of (A) non-stretched human LECs, (B-D) stretched human LECs after transfection with (B) RLuc control siRNA, (C) β1 integrin siRNA-1, or (D) VEGFR3 siRNA-1, and incubated with BrdU to analyse cell proliferation. The LECs were fixed after removal from the stretching chamber, and immunostained to visualize the incorporation of BrdU (green) and the nuclei (DAPI, blue). Scale bars, 100 μm.

(E) Increase in BrdU incorporation in LECs that were non-stretched (white columns), stretched (black columns) or stretched after β1 integrin or VEGFR3 silencing (grey columns). LECs were transfected with control siRNA, β1 integrin siRNA-1, β1 integrin siRNA-2 targeting the 3'-UTR, β1 integrin siRNA-2 together with a 3'-EGFP-β1 integrin expression vector (β1 integrin rescue), VEGFR3 siRNA-1, VEGFR3 siRNA-2 targeting the 3'-UTR, or VEGFR3 siRNA-2 together with a vector expressing VEGFR3 without 3'-UTR (VEGFR3 rescue). Immunostaining was performed after 30 minutes stretching and BrdU incorporation. All values are means ± SD, $n \geq 3$ experiments, $^*p < 0.05$ (first bracket: $p = 0.005$, second bracket: $p = 0.009$, third bracket: $p = 0.001$, lower brackets: $p = 0.002$ and $p = 0.042$, fourth bracket: $p = 0.020$, fifth bracket: $p = 0.002$, sixth bracket: $p = 0.038$, uppermost brackets: $p = 0.002$, $p = 0.0006$, $p = 0.036$).

Supplementary Figure S12: Stretching LECs does not increase VEGF-C mRNA expression.

(A) RT-PCR products for Vegf-c and β-actin in human LECs that were non-stretched or stretched. The breast cancer cell line MDA-MB-231 was used as positive control.

(B) Vegf-c mRNA expression normalised to β-actin mRNA expression of human LECs that were non-stretched (white column) or stretched (black column), and of breast cancer MDA-MB-231 cells (grey column) shown in (A). A.U.: arbitrary units. All values are means ± SD, n = 3 experiments per condition, ns = non-significant (p = 0.238).

Supplementary Figure S13: β1 integrin deletion in LECs.

(A-D) β-galactosidase immunostaining of cross-sections through the jugular lymph sac (jls) of an E12.5 mouse embryo harbouring an Vegfr2/Flk1-Cre transgene and a Cre reporter. Arrowheads point to a vascular endothelial cell, which does not stain for the lymphatic marker Lyve-1 (green). Arrows point to a macrophage, which expresses Lyve-1 (green), but not PECAM-1 (red), and does not stain for β-galactosidase (grey). Scale bars, 20 μm.

(E-J) Cross-sections through jugular lymph sacs (jls) of (E-G) β1 integrin$^{\Delta/+}$ control E11.5 embryos and (H-J) β1 integrin$^{\Delta/\Delta}$ E11.5 embryos, immunostained for (E, H) Lyve-1 and (F, I) β1 integrin. (G, J) Merged colours with cell nuclei (DAPI, blue). Note the absence of β1 integrin in LECs of β1 integrin$^{\Delta/\Delta}$ mouse embryos. Scale bars, 10 μm.

(K) β1 integrin mRNA expression as determined by real-time RT-PCR of LECs sorted from β1 integrin$^{\Delta/+}$ (black column) and β1 integrin$^{\Delta/\Delta}$ (white column) E12.0-E12.5 mouse embryos. All values are means ± SD, n ≥ 5 mouse embryos per genotype, *p = 0.0005.

(L) RT-PCR products for β1 integrin and β2-microglobulin of LECs sorted from β1 integrin$^{\Delta/+}$ and β1 integrin$^{\Delta/\Delta}$ E12.0-E12.5 mouse embryos. Total RNA from an E12.5 wild type embryo was used as positive control. The lower graph shows β1 integrin mRNA expression normalised to β2-microglobulin mRNA expression of sorted LECs from β1 integrin$^{\Delta/+}$ (black columns) and β1 integrin$^{\Delta/\Delta}$ (white columns) E12.0-E12.5 mouse embryos, and of an E12.5 wild type embryo (grey column). A.U.: arbitrary units.

Supplementary Figure S14: β1 integrin deletion in LECs leads to oedema, embryonic death and absence of lymph vessels.

(A) Table showing (1) the total numbers of analysed mice, (2) numbers of mice with homozygous deletion of β1 integrin (β1 integrin$^{\Delta/\Delta}$), and (3) numbers of β1 integrin$^{\Delta/\Delta}$ mice that contain oedema.

(B-G) Representative images of (B-D) β1 integrin$^{\Delta/+}$ and (E-G) β1 integrin$^{\Delta/\Delta}$ E15.5 mouse embryos immunostained for Lyve-1 (in B, C, E, F, green; in D, G, brown). Arrows (B-D) point to lymph vessels in the β1 integrin$^{\Delta/+}$ mouse embryos. Note the absence of Lyve-1^{+} lymph vessels in the β1 integrin$^{\Delta/\Delta}$ mice. Scattered Lyve-1^{+} cells most likely represent macrophages. Scale bars, 100 μm.

Supplementary Figure S15: β1 integrin is not required for LEC survival during early lymphatic development.

(A, A', B, B') Cross-sections through the jugular lymph sac (jls) of (A) a representative β1 integrin$^{\Delta/+}$ control E11.5 mouse embryo and (B) a β1 integrin$^{\Delta/\Delta}$ E11.5 mouse embryo immunostained for Lyve-1 (green), apoptosis marker Caspase-3 (red) and nuclei (DAPI, blue). Some apoptotic cells are magnified in (A') and (B'). Scale bars, (A, B) 100 μm, (A', B') 20 μm.

(C) Quantification of the numbers of apoptotic LECs in mouse embryos harbouring a heterozygous (black columns) or homozygous (white columns) deletion of β1 integrin. All values are means ± SD, n ≥ 3 embryos per genotype and stage.

Supplementary Movie S1. Measurement of interstitial fluid pressure.

The movie shows a glass capillary inserted into the jugular mesenchyme of an E11.5 and an E12.0 mouse embryo. Note the different volumes of interstitial fluid entering the capillary.

Supplementary Movie S2. Whole embryo cultivation (WEC) for 12 hours.

The movie shows an embryo isolated at E11.5 and an E11.5 embryo after cultivation in WEC for 12 hours. After 12 hours in WEC, the embryo still had a beating heart and appeared vital.

Planas-Paz_Supplementary Figure S1

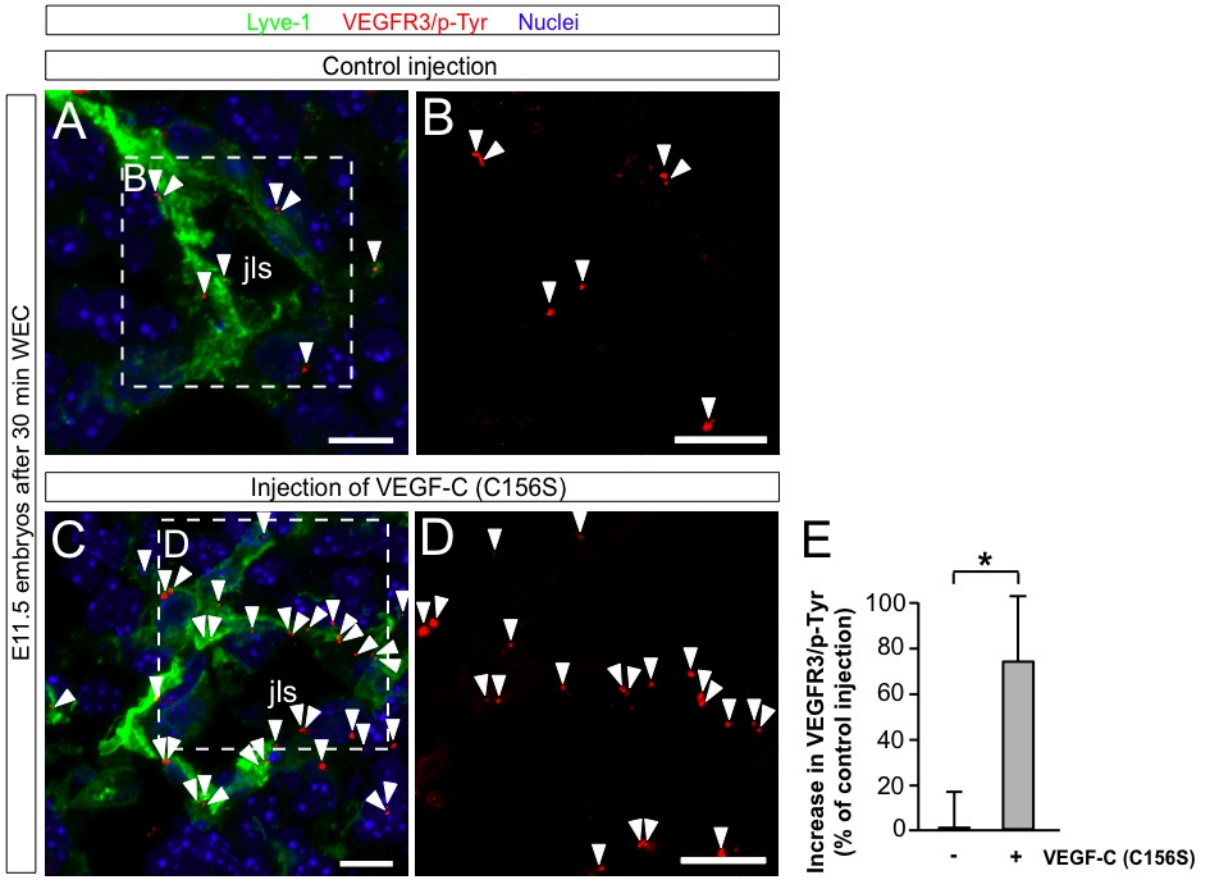

Planas-Paz_Supplementary Figure S2

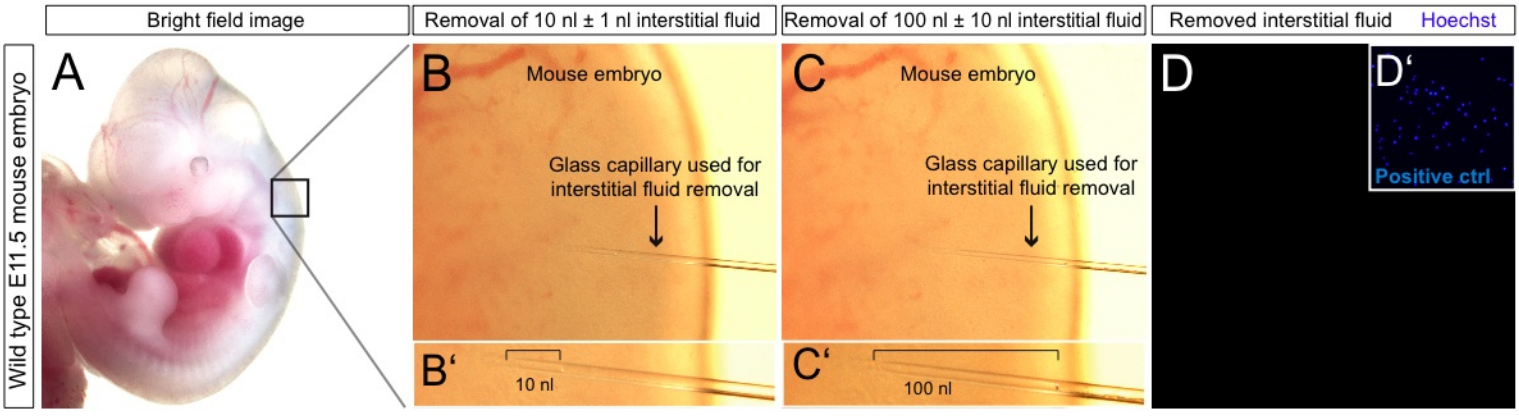

Planas-Paz_Supplementary Figure S3

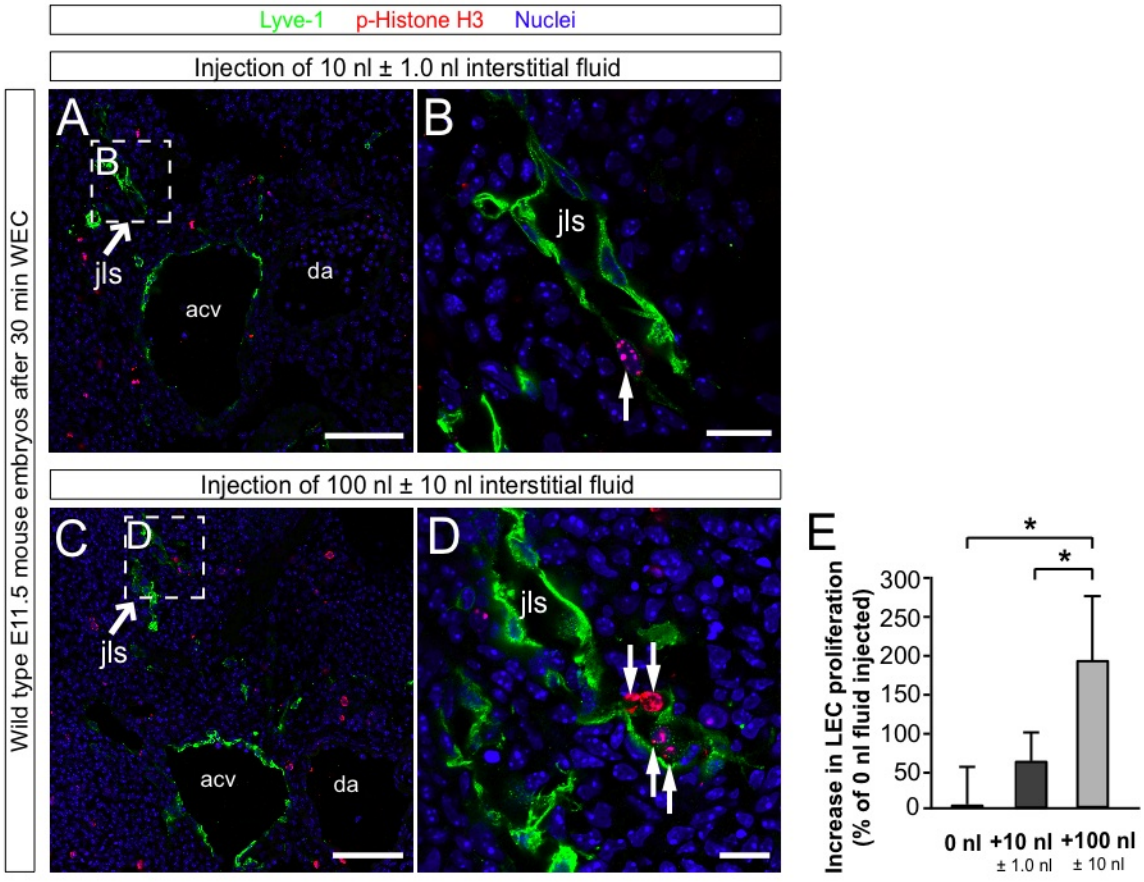

Planas-Paz_Supplementary Figure S4

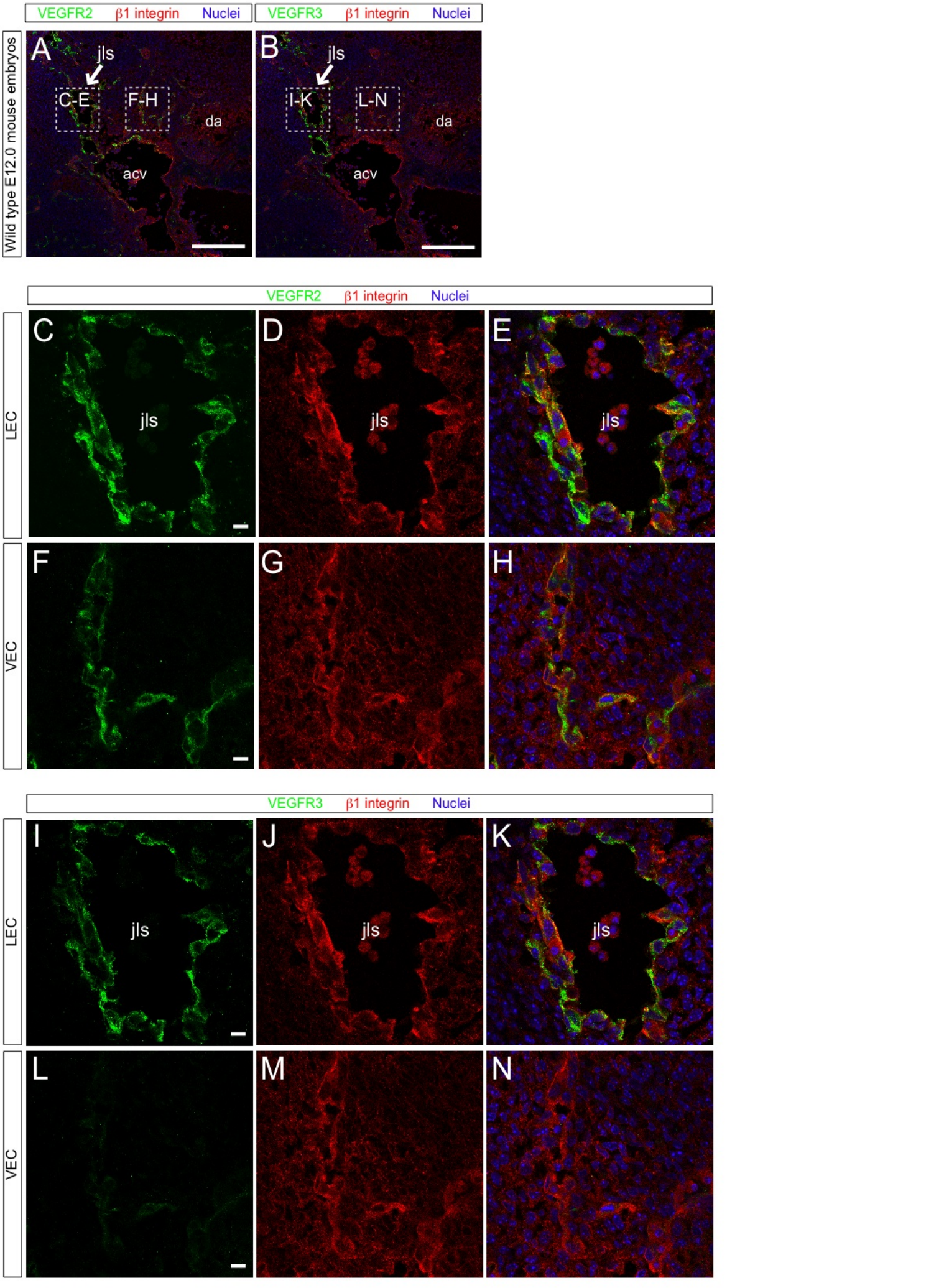

Planas-Paz_Supplementary Figure S5

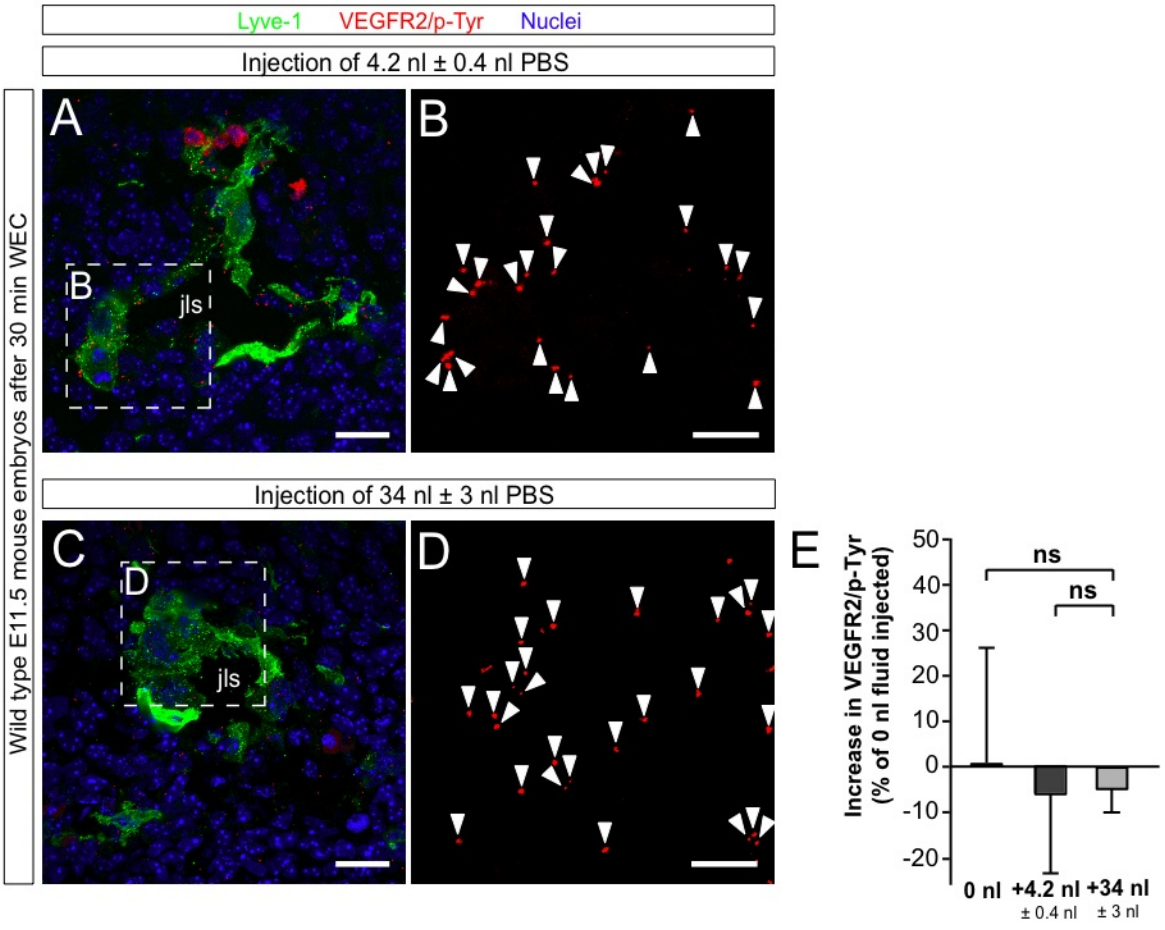

Planas-Paz_Supplementary Figure S6

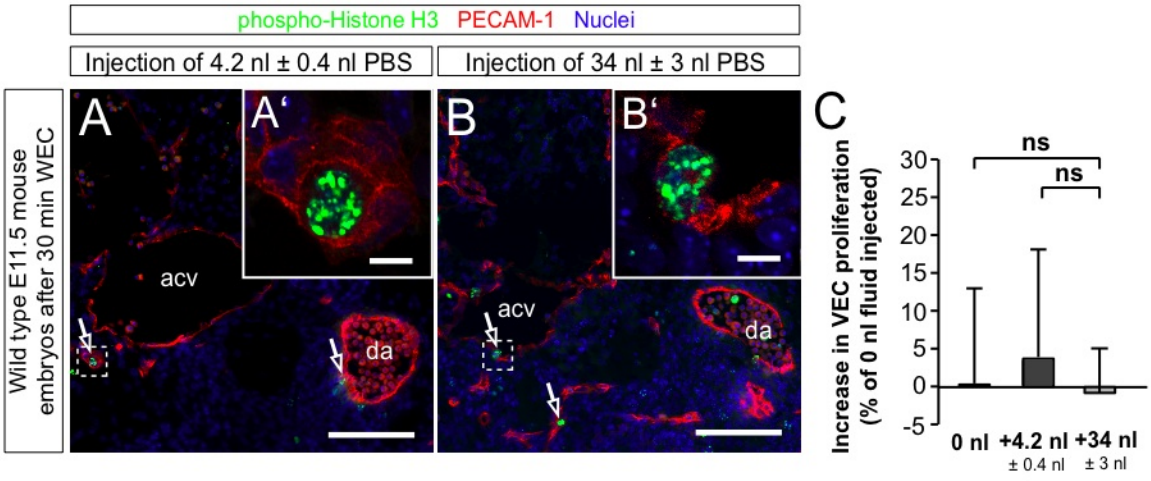

Planas-Paz_Supplementary Figure S7

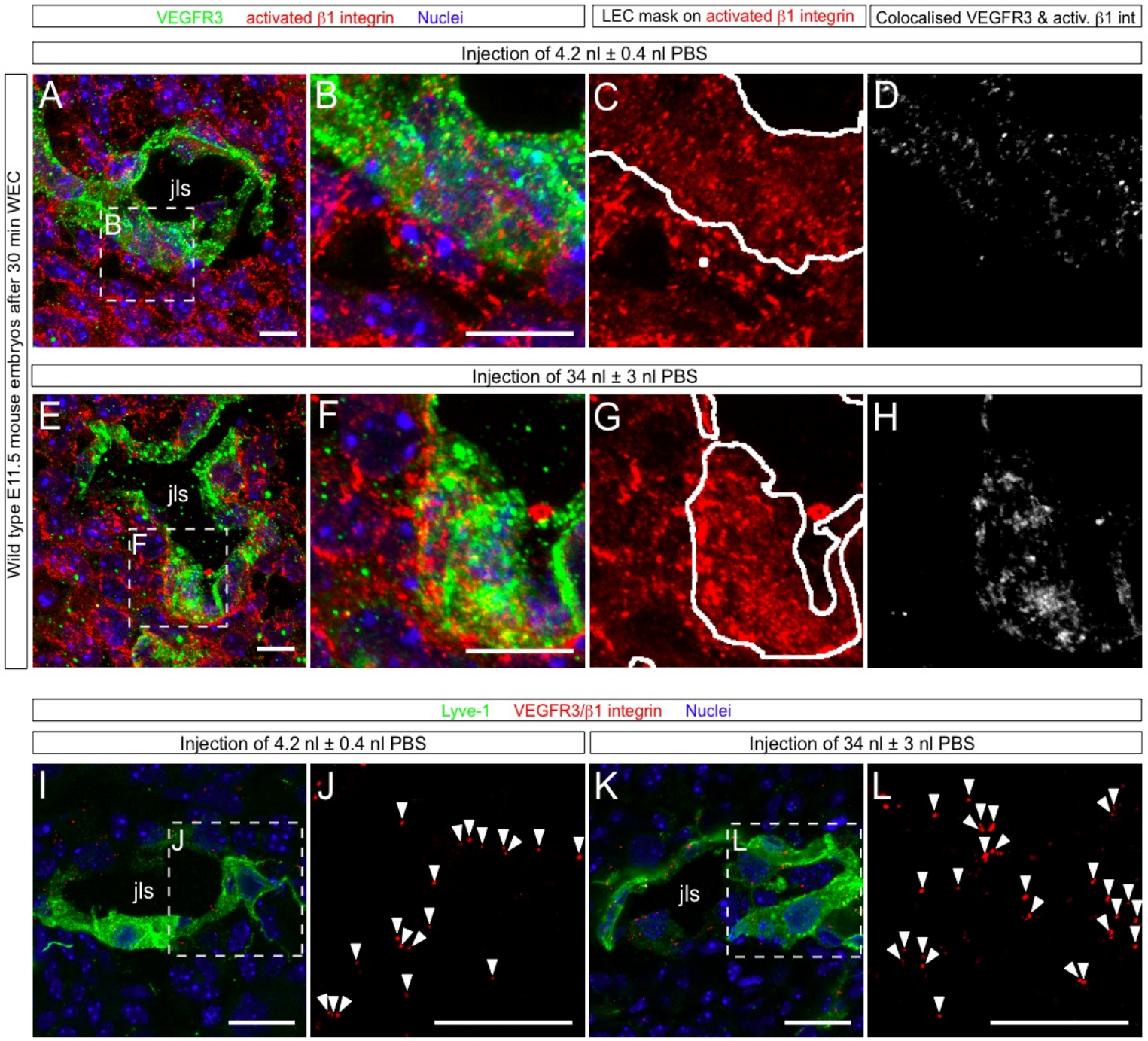

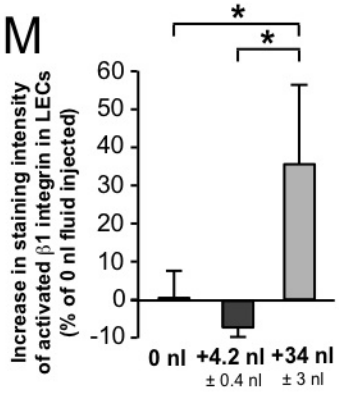

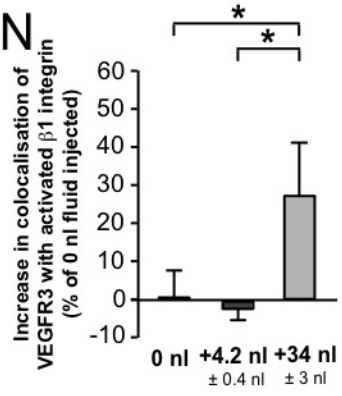

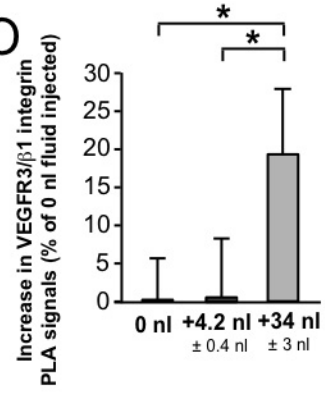

Planas-Paz_Supplementary Figure S8

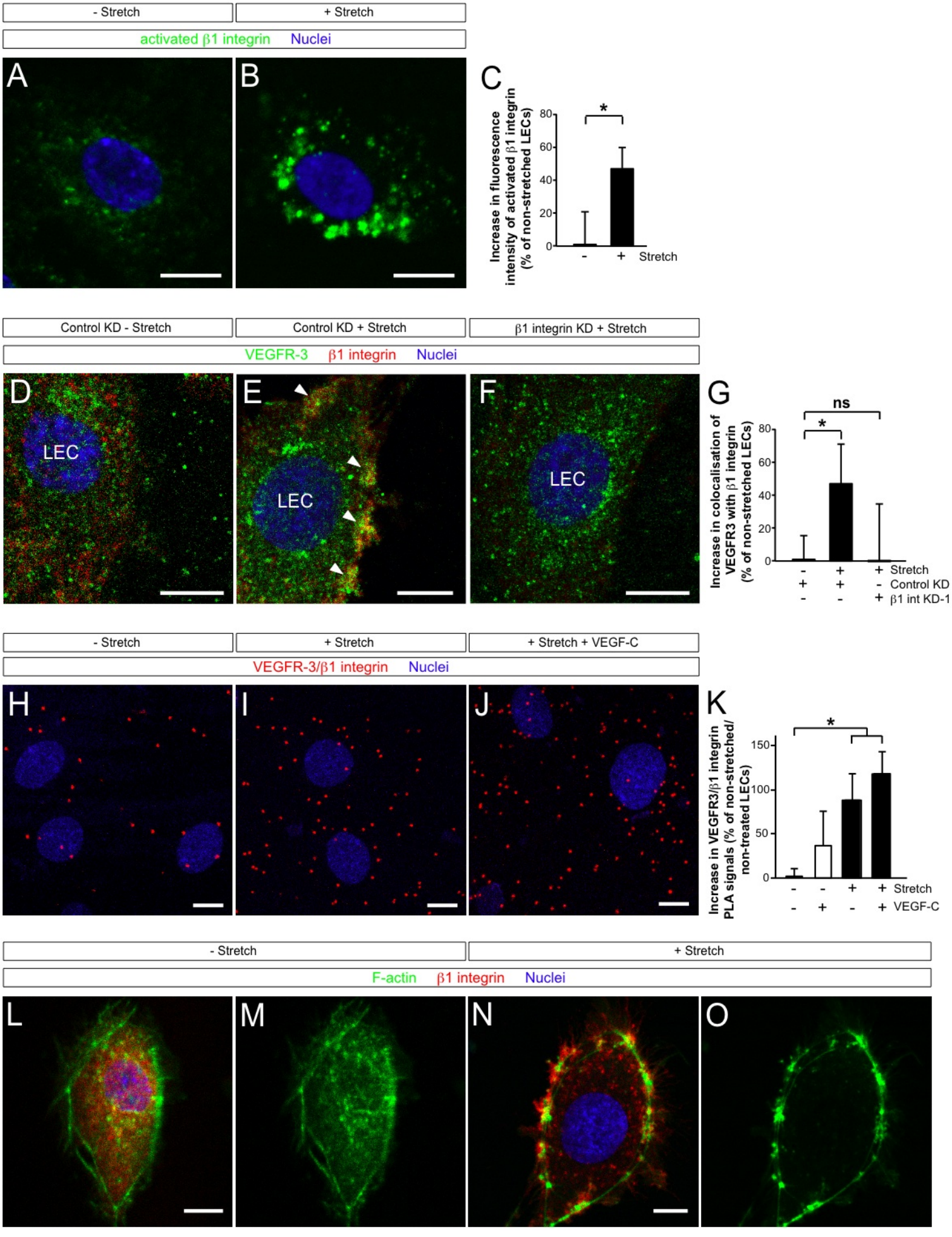

Planas-Paz_Supplementary Figure S9

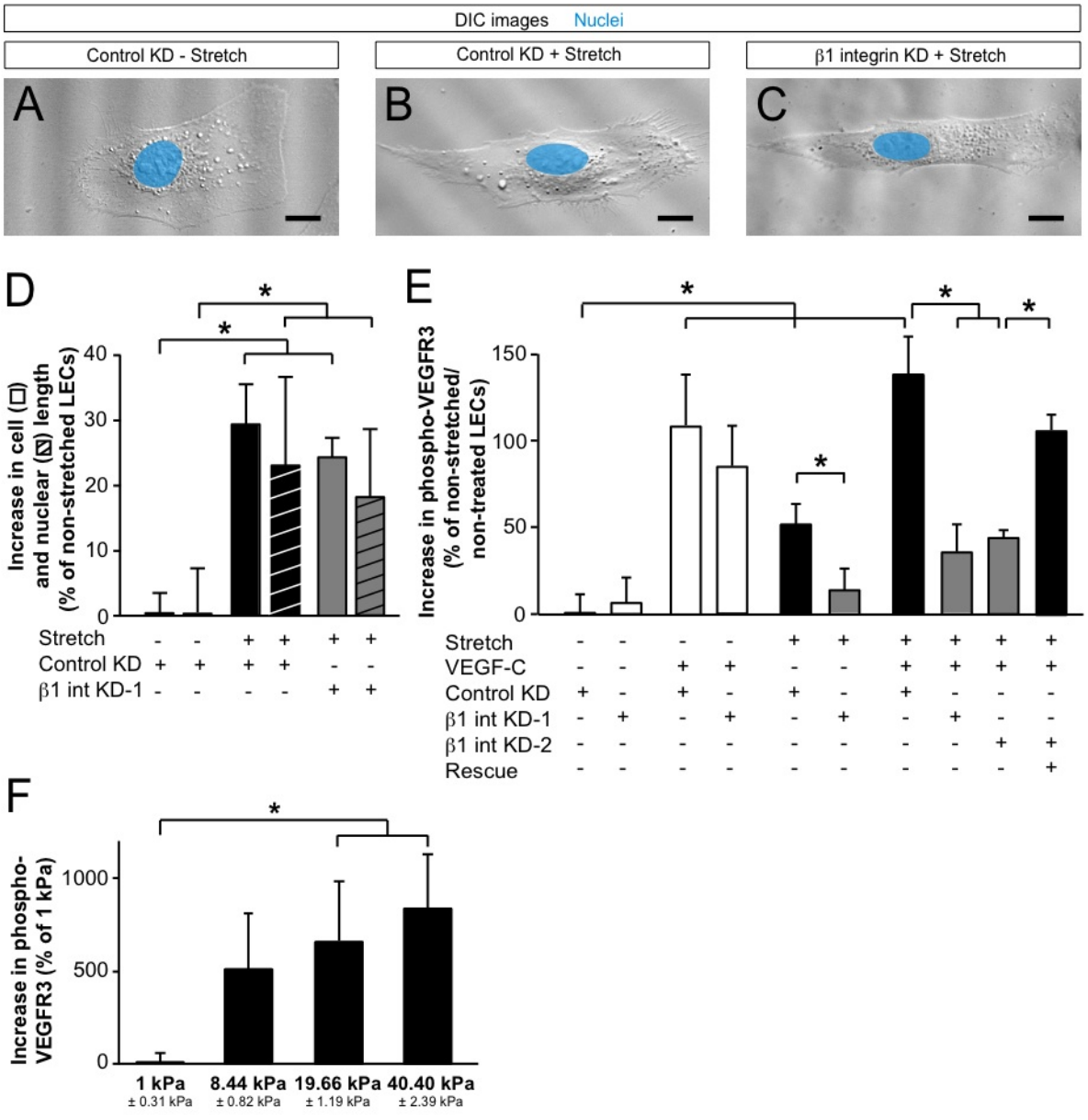

Planas-Paz_Supplementary Figure S10

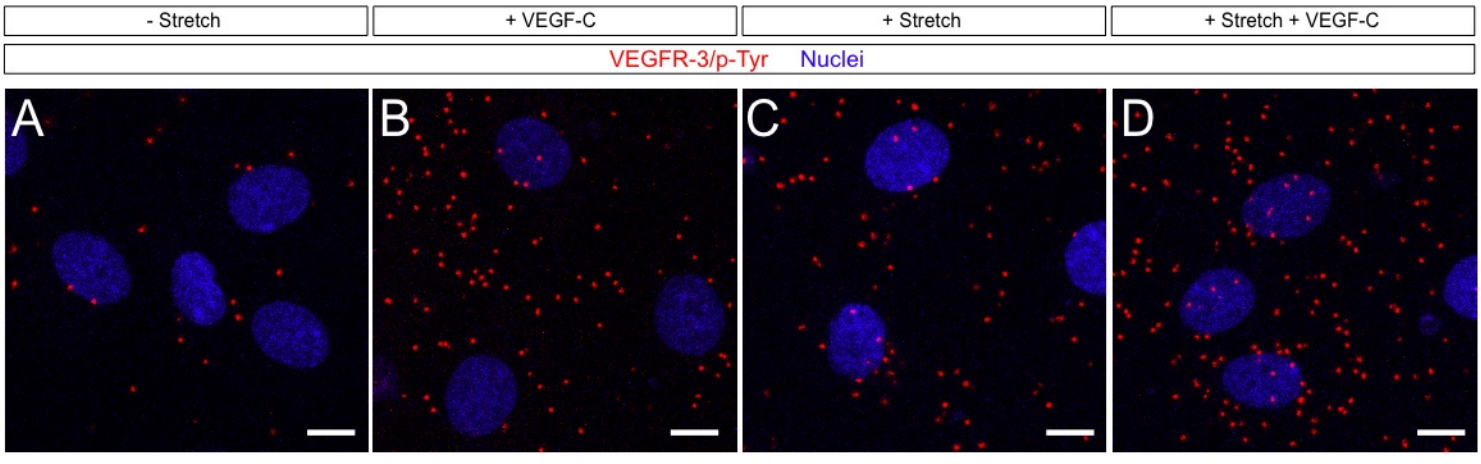

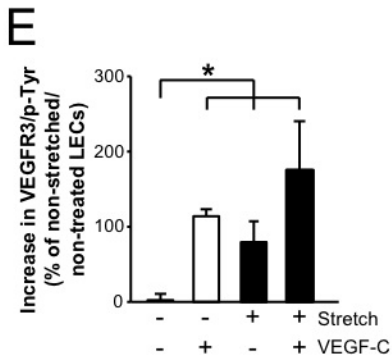

Planas-Paz_Supplementary Figure S11

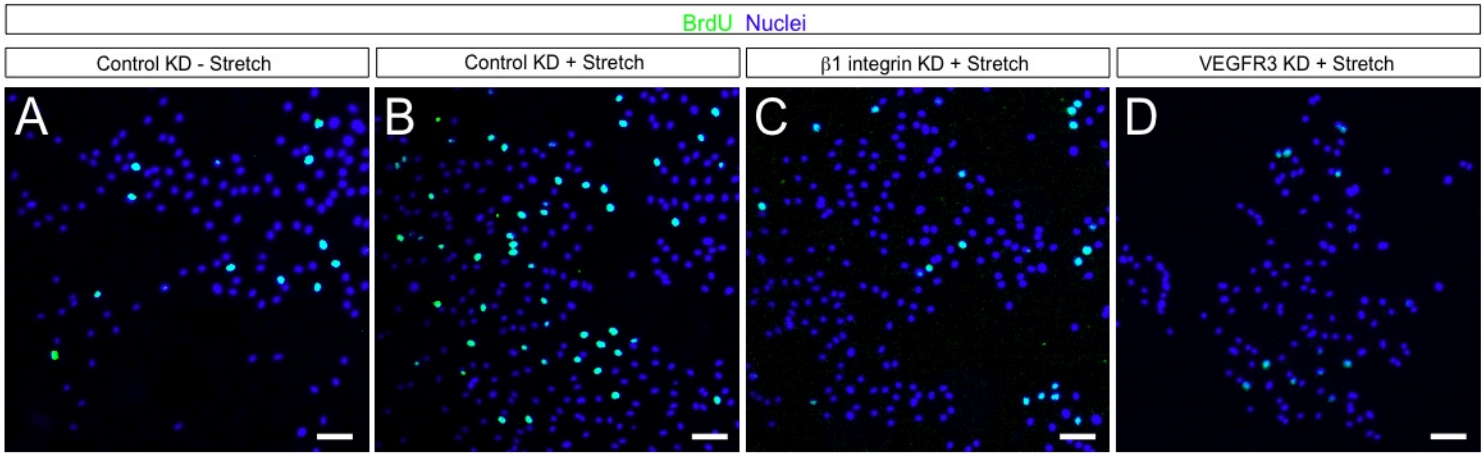

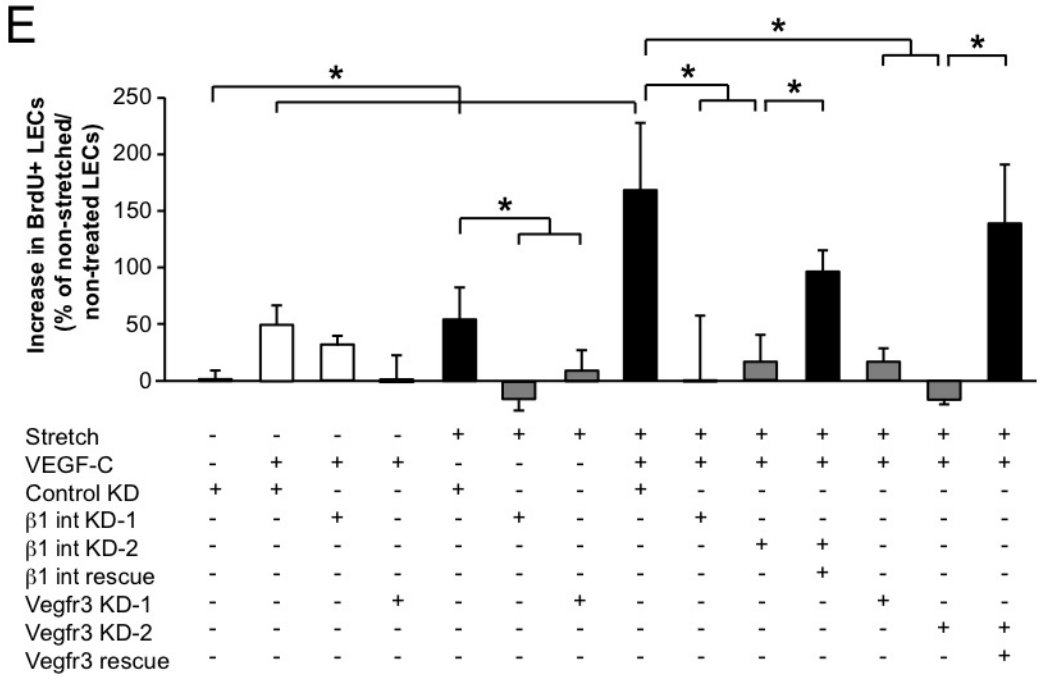

Planas-Paz_Supplementary Figure S12

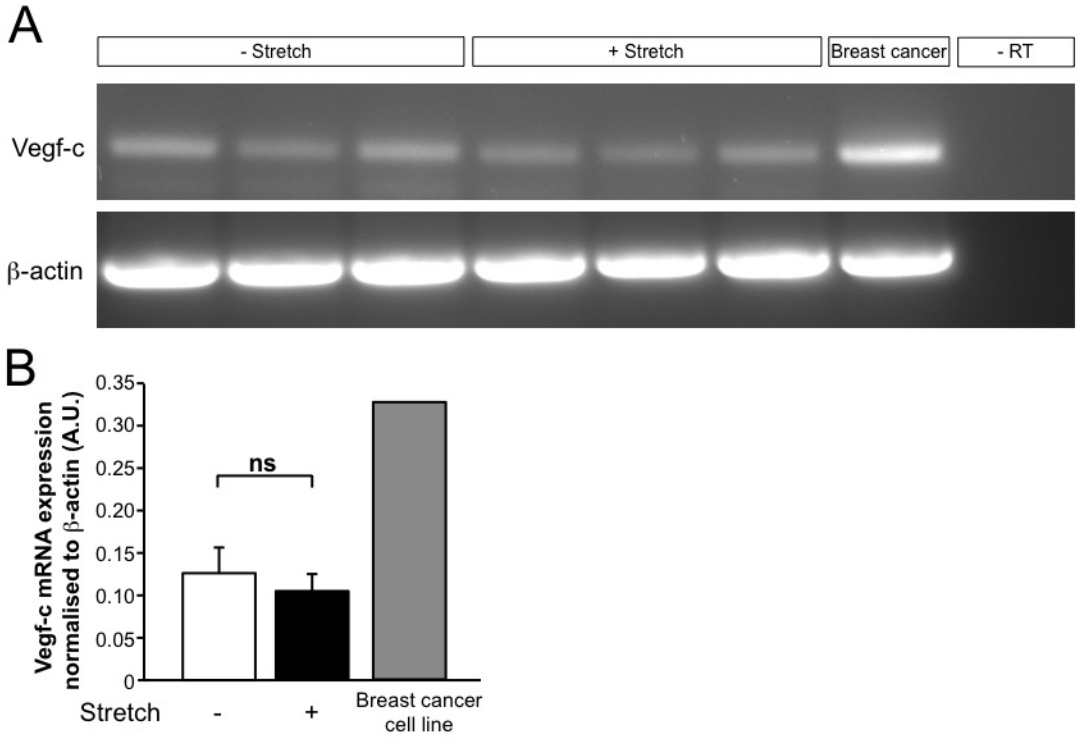

Planas-Paz_Supplementary Figure S13

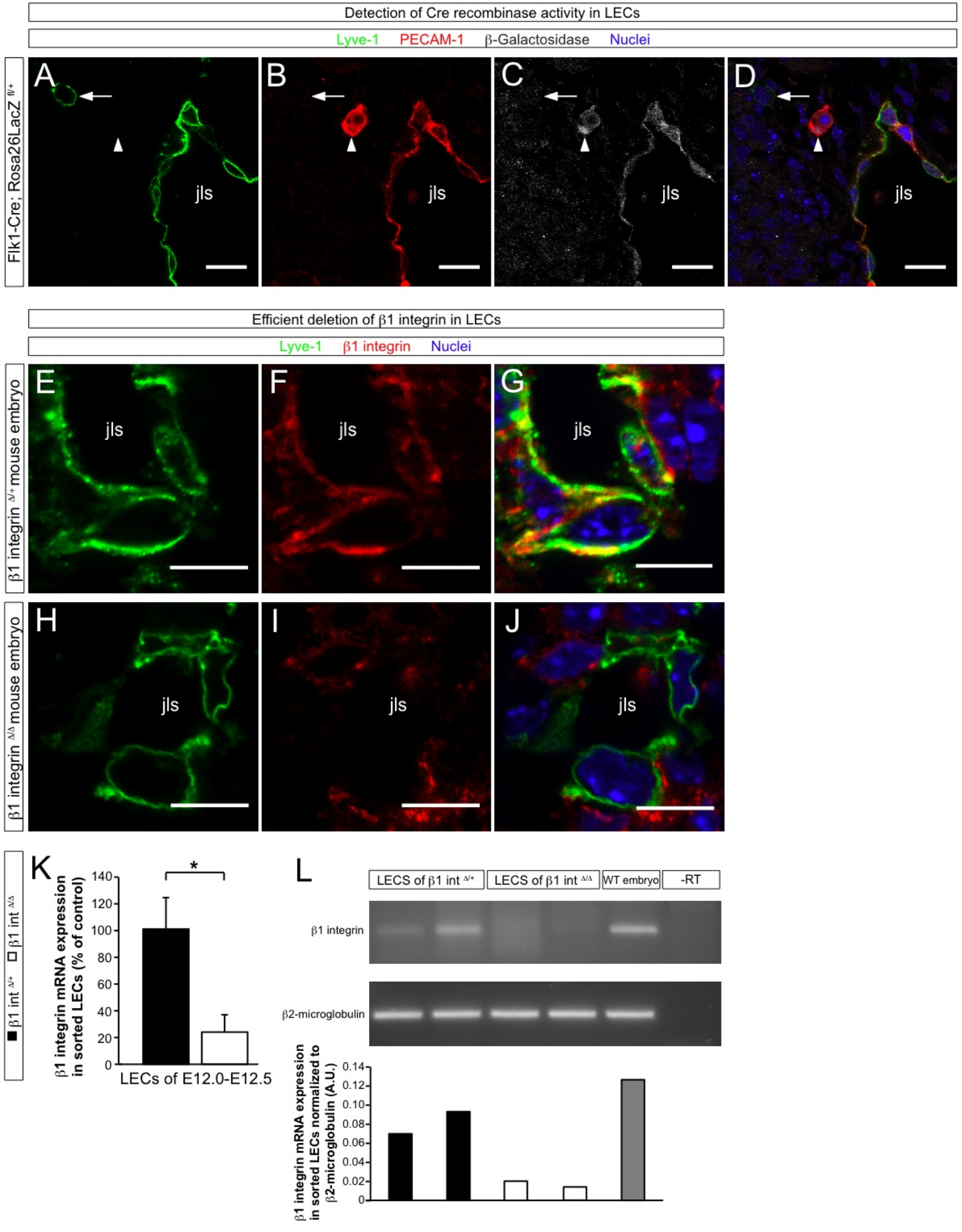

Planas-Paz_Supplementary Figure S14

A

Stage analysed	E11.5	E13.5	E15.5	P1
(1) # Embryos analysed	191	73	67	48
(2) # β1 integrin $^{\Delta/\Delta}$ embryos (% of total # embryos)	57 (30%)	23 (32%)	15 (22%)	0 (0%)
(3) # β1 integrin $^{\Delta/\Delta}$ embryos with oedema (% of all β1 integrin $^{\Delta/\Delta}$ embryos)	0 (0%)	15 (65%)	12 (80%)	

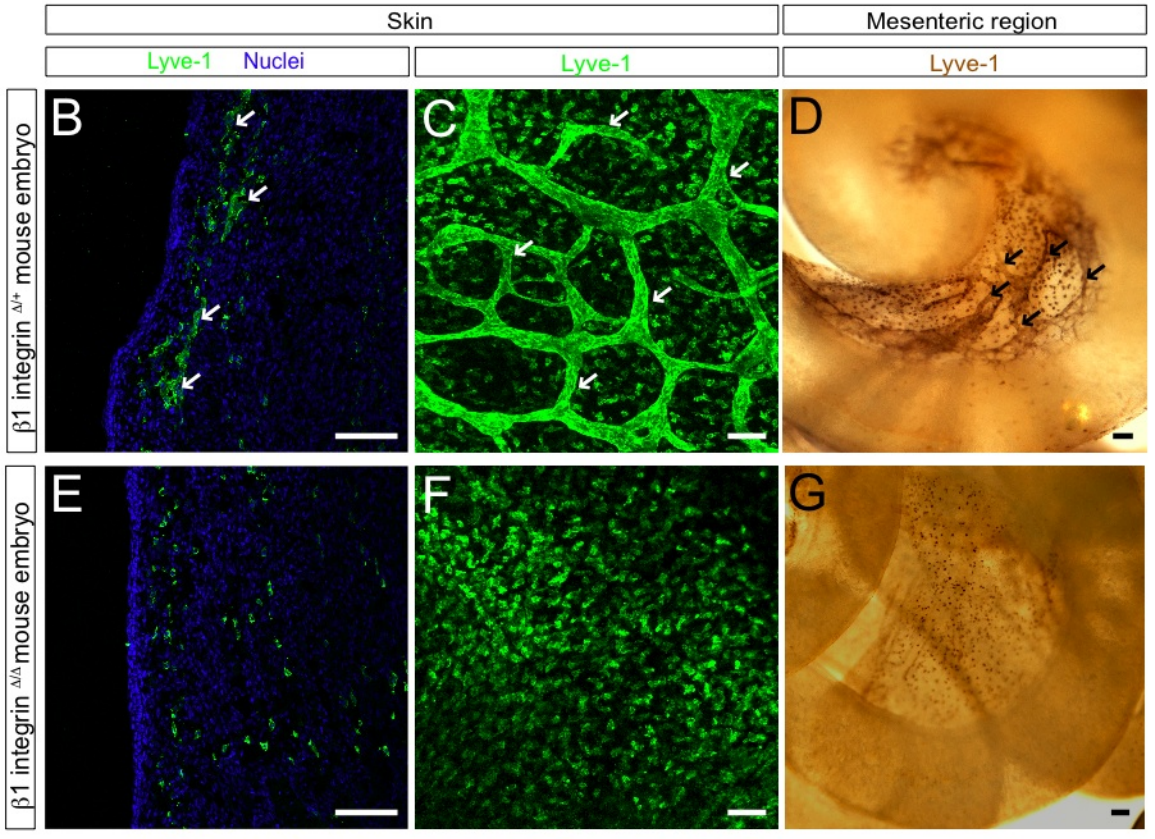

Planas-Paz_Supplementary Figure S15